

Vortex dynamics in Co-Fe-B magnetic tunnel junctions in presence of defects

M. Kuepferling, S. Zullino, A. Sola, B. Van de Wiele, G. Durin, M. Pasquale, K. Rott, G. Reiss, and G. Bertotti

Citation: *Journal of Applied Physics* **117**, 17E107 (2015); doi: 10.1063/1.4908142

View online: <http://dx.doi.org/10.1063/1.4908142>

View Table of Contents: <http://scitation.aip.org/content/aip/journal/jap/117/17?ver=pdfcov>

Published by the [AIP Publishing](#)

Articles you may be interested in

[Perpendicular magnetic tunnel junctions based on thin CoFeB free layer and Co-based multilayer synthetic antiferromagnet pinned layers](#)

J. Appl. Phys. **111**, 07C918 (2012); 10.1063/1.3679432

[Reduction of switching current density in perpendicular magnetic tunnel junctions by tuning the anisotropy of the CoFeB free layer](#)

J. Appl. Phys. **111**, 07C907 (2012); 10.1063/1.3673834

[Ferromagnetic resonance and damping properties of CoFeB thin films as free layers in MgO-based magnetic tunnel junctions](#)

J. Appl. Phys. **110**, 033910 (2011); 10.1063/1.3615961

[Effects of Co addition on magneto-transport properties of magnetic tunnel junction consisting of CoFeB or CoFeSiB free layer](#)

J. Appl. Phys. **109**, 07D346 (2011); 10.1063/1.3565404

[230% room-temperature magnetoresistance in CoFeB/MgO/CoFeB magnetic tunnel junctions](#)

Appl. Phys. Lett. **86**, 092502 (2005); 10.1063/1.1871344



You don't still use this cell phone

or this computer

Why are you still using an AFM designed in the 80's?

It is time to upgrade your AFM

Minimum \$20,000 trade-in discount for purchases before August 31st

Asylum Research is today's technology leader in AFM

dropmyoldAFM@oxinst.com

OXFORD
INSTRUMENTS
The Business of Science®

Vortex dynamics in Co-Fe-B magnetic tunnel junctions in presence of defects

M. Kuepferling,^{1,a)} S. Zullino,¹ A. Sola,¹ B. Van de Wiele,² G. Durin,^{1,3} M. Pasquale,¹ K. Rott,⁴ G. Reiss,⁴ and G. Bertotti¹

¹*Istituto Nazionale di Ricerca Metrologica (INRIM), Strada delle Cacce 91, 10135 Turin, Italy*

²*Department of Electrical Energy, Systems and Automation, Ghent University, Technologiepark 914, B-9052 Ghent-Zwijnaarde, Belgium*

³*ISI Foundation, via Alassio 11/c, 10126 Turin, Italy*

⁴*Physics Department, Bielefeld University, P.O. Box 100131, 33501 Bielefeld, Germany*

(Presented 5 November 2014; received 22 September 2014; accepted 16 October 2014; published online 13 February 2015)

We investigate the frequency of thermally excited vortex oscillations in Co-Fe-B magnetic tunnel junction (MTJ) pillars in the presence of defects. Under a variable in-plane magnetic field, a characteristic behavior is observed: the frequency oscillates from a maximum at certain field values to a steep minimum, which tends towards zero frequency. These frequency variations are described qualitatively well by an analytical model based on the Thiele equation taking into account a single Gaussian pinning potential. It is thus possible to calculate the in-plane depinning field for certain pinning potential parameters. For steep potentials, the depinning is hysteretic and jumps between the pinned and unpinned regime occur due to the presence of an energy barrier. A sharp frequency minimum occurs at an applied field, where a large flat region in the energy landscape is present. From the experiments, the pinning potentials are estimated to be between -0.2eV and -0.4eV . We also perform micromagnetic simulations of the vortex oscillations in the presence of a distribution of pinning centers. The simulations confirm the validity of the Thiele-approach showing that the vortex remains sufficiently rigid. © 2015 AIP Publishing LLC.

[<http://dx.doi.org/10.1063/1.4908142>]

I. INTRODUCTION

Defects can modify substantially the magnetic response of ferromagnetic materials. In models, they are often taken into account as statistic distribution of pinning potentials that modify the domain wall motion, leading to hysteresis and Barkhausen jumps. A problem arises when ferromagnetic nanostructures are considered. In this case, statistic models cannot be applied and often the micromagnetic approach has to be adopted.^{1,2} Due to the complexity of the problem, assumptions have to be made about the nature of the defects and how they interact with the domain wall. There is a renewed interest in the influence of defects on the domain wall dynamics, due to its importance in the proposed race-track memories, which exploit the domain wall motion in nanowires.³

Simple problems help to obtain a better comprehension of the influence of defects on domain wall dynamics. In particular, the vortex dynamics has received a growing interest, since it can be described as a rigid magnetic configuration by a single parameter.⁴ It is important in nanowires, being energetically more stable than the transverse wall for large wire cross-sections (vortex wall),⁵ as well as in disks. In vortex domain walls, core switches can occur at material defects,⁶ while in nano-disks the magnetic vortex configuration was employed to probe single defects.^{7,8} It is therefore important

to understand if the vortex interacts rigidly or point-like with defects, so that simple analytic models can be applied.

Despite the many analogies between domain walls in wires and vortices in disks, it was found that the vortex dynamics in disks is less influenced by defects than a domain wall in a nanowire.⁹ In particular, an increased damping was found for current-induced domain wall motion including defects,¹ while the pinned vortex essentially exhibits comparable damping as the non-pinned vortex.⁹ While the field or current-driven vortex wall has to overcome potential wells and move from one pinning center to the next, the vortex trapped in a pinning center oscillates at a higher frequency due to the steeper potential.

In this paper, we investigate a gyrating vortex that moves between different pinning centers driven by an applied magnetic field. To this aim, we measured vortex oscillations in Co-Fe-B magnetic tunnel junction (MTJ) pillars in the presence of defects. We thus aim to obtain a better understanding of the particular frequency versus field behavior observed experimentally with focus on the depinning driven by the field. While previously the low frequency/high power oscillations were attributed to flat pinning potentials,¹⁰ we find that they correspond to flat regions in the energy landscape accompanied by large-amplitude high power oscillations during the depinning. Analytically this depinning driven by the field can be hysteretic or non-hysteretic, depending on the steepness of the pinning potential. We also perform micromagnetic simulations with a distribution of grains which substantially confirm the

^{a)}Electronic mail: m.kuepferling@inrim.it.

dynamics. We then characterize the experimentally observed defects obtaining the typical pinning potential amplitude and radius.

II. EXPERIMENTAL

MTJs are optimal magnetic devices to investigate vortex oscillations. Due to the tunnel magneto-resistance effect (TMR), even small power vortex oscillations, caused by thermal fluctuations, are measurable.¹⁰ The samples investigated were prepared at the University of Bielefeld by sputter deposition. A multilayer stack $\text{Mn}_{83}\text{Ir}_{17}$ (12 nm)/ $\text{Co}_{40}\text{Fe}_{40}\text{B}_{20}$ (3 nm)/ MgO (1.1 nm)/ $\text{Co}_{40}\text{Fe}_{40}\text{B}_{20}$ (2 nm)/ $\text{Ni}_{81}\text{Fe}_{19}$ (30 nm) was patterned into pillars with circular cross section of diameters of 460 nm, 590 nm, and 780 nm. The polarizer $\text{Co}_{40}\text{Fe}_{40}\text{B}_{20}$ (3 nm) is pinned by exchange bias to the antiferromagnetic $\text{Mn}_{83}\text{Ir}_{17}$ layer. The free layer consists of a $\text{Co}_{40}\text{Fe}_{40}\text{B}_{20}$ layer (2 nm), which enhances the TMR and a thick $\text{Ni}_{81}\text{Fe}_{19}$ (Py) layer (30 nm), which favors the formation of a vortex magnetization configuration. Each stack has been annealed before patterning in an in-plane field of 0.6 T at 360 °C in order to have a well-defined in-plane anisotropy of the polarizer layer and to form a tunnel junction with large TMR.¹¹

Measurements of magnetization oscillations were performed using an Agilent spectrum analyzer (3 Hz–50 GHz). The magnetic field was applied by an electromagnet. Magnetization oscillations were measured via TMR with an applied DC current perpendicular-to-plane (cpp) between 1 mA and 3 mA, where positive current means electrons flowing from the fixed to the free layer. These currents are well below the critical breakdown current for spin-torque vortex oscillations, estimated using the Thiele approach with a two-vortex-ansatz,^{12,13} to be approximately 25 mA for the device with 590 nm diameter. The DC current favors the excitation of thermal vortex oscillations, since it reduces the damping and slightly increases the sample temperature. Power spectra were measured in a range of 10–1000 MHz using 1200 points and 100 averages.

Fig. 1 shows oscillation frequency versus field applied in the sample plane parallel to the pinning direction. The vortex oscillations occur at increasing fields at -14 mT and disappear at -44 mT for decreasing field (device with diameter 590 nm). This field range corresponds to the nucleation and annihilation fields of the vortex. The frequency shows the characteristic behavior of thermally excited vortex oscillations: the frequency is oscillating between a maximum value

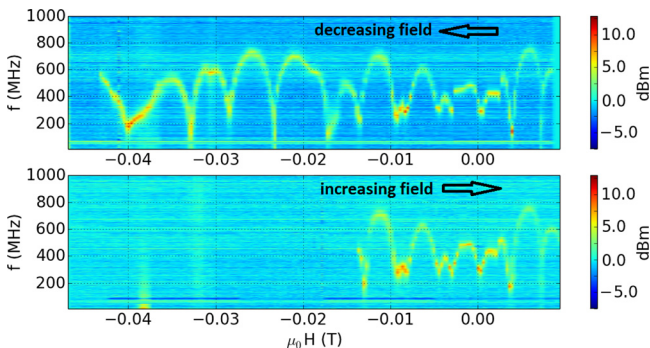


FIG. 1. Field sweep in small field range: at certain field values, steep minima in frequency are present ($I_{DC} = 3$ mA and diameter of device = 590 nm).

of ~ 790 MHz and minima that reach very low values of 10 MHz. Once the vortex is nucleated, the frequency versus field diagrams coincides for increasing and decreasing field. The frequency maxima correspond presumably to different pinning centers along a line perpendicular to the applied magnetic field, which displaces the vortex. The average $\Delta\mu_0 H$ between the minima is 1.3 mT ($d = 780$ nm), 2.4 mT ($d = 590$ nm), and 3.3 mT ($d = 460$ nm). Detailed field sweeps (small field range) were performed and while the frequency behavior is perfectly reproducible, no hysteresis was observable between increasing and decreasing field (see Fig. 2).

III. DISCUSSION

The experimental results were compared with micro-magnetic simulations and an analytical model based on the Thiele equation with the two-vortices-ansatz.¹²

A. Analytical model

The frequency of vortex oscillations in a circular disk can be calculated analytically assuming that the motion can be described only by the displacement of the center of the vortex (vortex core position $\vec{X}_0 = \vec{X}_0(t)$), i.e., translational mode of the vortex

$$|\vec{G}| \frac{d}{dt} \vec{X}_0 = \hat{e}_z \times \frac{\partial W}{\partial \vec{X}_0}. \quad (1)$$

where \vec{G} is the gyrovector given by $\frac{2\pi p d M_s}{\gamma} \hat{e}_z$ (p is the polarity of the vortex, γ is the gyromagnetic ratio, d is the thickness of the layer, and M_s is the saturation magnetization).

The fact that the disk confines the vortex configuration needs to be considered in the vortex energy W by the two-vortices ansatz. In this way, the magnetization is always tangential at the disk border. The vortex energy in the presence of a magnetic field and a DC current I , generating an Oersted field, is then given by

$$W = \mu_0 M_s^2 \frac{d^2}{R} \frac{10}{9} \frac{1}{2} |\vec{X}_0|^2 + \frac{2}{15} \mu_0 M_s \frac{d}{R} I |\vec{X}_0|^2 - \frac{2}{3} \mu_0 \pi M_s d R H X_0, \quad (2)$$

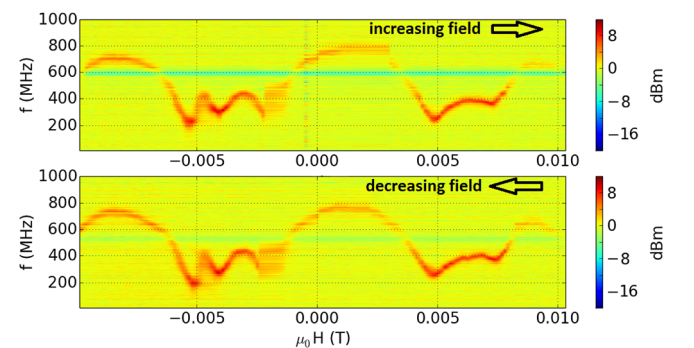


FIG. 2. Field sweep showing only few frequency minima and maxima ($I_{DC} = 1.8$ mA and diameter of device = 460 nm). No hysteresis is observable.

where the first term is the dipolar magnetostatic energy in a disk with radius R , the second is the Zeeman energy of the vortex configuration in the Oersted field, and the third is the Zeeman energy in the applied magnetic field $\vec{H} = H\hat{e}_y$. In the following, for Py a value of $\mu_0 M_s = 0.9$ T is used.

The energy minimum defines the field dependent equilibrium position and the shape of the energy potential (steepness) defines the slightly current dependent oscillation frequency. For example, the oscillation frequency in the Py disk of 590 nm diameter is 453 MHz at zero DC current, the frequency change due to the Oersted field at 3 mA DC current is 15 MHz. From the derivative of the field dependent energy the equilibrium position can be calculated, which is linear in field. For the experimental sample diameters, the following values for the vortex displacement with field are calculated: 3.9 nm/mT ($d = 460$ nm), 4.6 nm/mT ($d = 590$ nm), and 5.7 nm/mT ($d = 780$ nm), which are in good agreement with previous results.⁸ Together with the experimental values of $\Delta\mu_0 H$ between the frequency minima, this leads to an average distance between the pinning centers of 13 nm ($d = 460$ nm), 11 nm ($d = 590$ nm), and 7 nm ($d = 780$ nm). These are only indicative values since in the presence of pinning centers the vortex displacement is not linear, but may exhibit sudden jumps (Barkhausen like).

The presence of pinning centers due to e.g., surface roughness (i.e., local changes of magnetization) or grain boundaries changes the energy landscape.^{7,14} Spatially confined energy minima located all over the Py disk have to be added to the energy W . The effect of a single pinning center on the oscillation frequency can be calculated by adding a Gaussian pinning potential to the vortex energy

$$W_p = -\frac{a}{q_e} e^{-\frac{|\vec{x}_0 - \vec{x}_p|^2}{c^2}}, \quad (3)$$

where a is the pinning strength in eV (q_e is the electron charge) and c is a measure for the extension of the potential in the plane. Typical values in literature are $0.3 \text{ eV} < a < 2 \text{ eV}$ and $5 \text{ nm} < c < 10 \text{ nm}$.¹⁴

Assuming that $\vec{X}_p = X_p \hat{e}_x$ when $\vec{H} = H\hat{e}_y$ means that the vortex core moves from the center of the disk and passes through the center of the pinning potential when the magnetic field is applied. From the minimum of the total energy, the vortex position can be calculated. It is found as the intersection of two functions (see Figure 3)

$$f_1(X_0) = -h, \quad (4)$$

$$f_2(X_0) = -(k_d + k_{oe})X_0 - a \frac{X_0 - X_p}{c^2 / \ln 2} e^{-\frac{(X_0 - X_p)^2}{c^2}}, \quad (5)$$

where $k_d = \mu_0 M_s^2 \frac{d^2}{R} \frac{10}{9}$, $k_{oe} = \mu_0 M_s \frac{d}{R} \frac{4}{15} I$ and $h = \frac{2}{3} \pi M_s d R B_{app}$. From Figure 3, we find that the vortex moves almost linearly with the applied field as long as its core is within a radius of c from the center of the pinning potential. This displacement is only small so that the vortex can be considered as pinned. At a certain field value A (here, 5.3 mT), a sudden jump occurs and the vortex core moves to position B , then continues a linear motion with field. When the field is decreased,

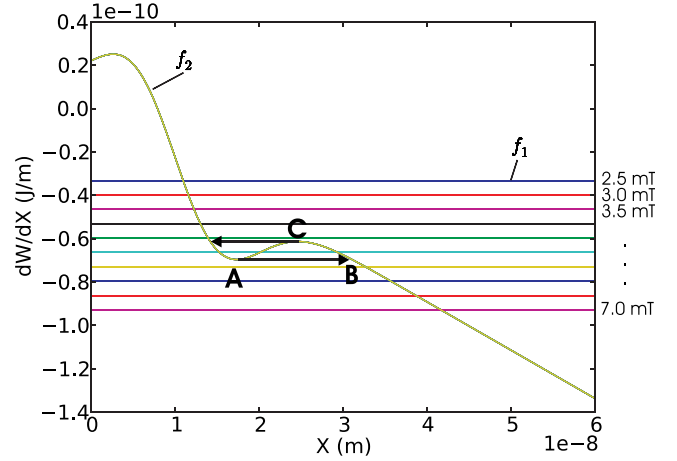


FIG. 3. The equilibrium position is given by the intersection of curves f_1 and f_2 as defined in Eqs. 4 and 5. The Gaussian pinning potential has the parameters $a = 2 \text{ eV}$ and $c = 7 \text{ nm}$.

the jump occurs at position C (hysteresis). From the plot, it is clear that the energy barrier does not always occur, but depends on the shape of the pinning potential with respect to the vortex energy. This is of special importance when the pinning potential is not steep (i.e., small a or large c). Then f_2 becomes very flat and the sum of the k values is large enough so that no energy barrier occurs. This limit is reached here for $a > -1.2 \text{ eV}$ or $c > 9 \text{ nm}$. This means that hysteresis is present only for pinning potentials that are steeper than these values. The fact that the experiment does not show hysteresis might indicate such pinning potentials. However, for a complete analysis, also thermal fluctuations have to be taken into account.¹⁵

For small motions around the equilibrium position, X_0 , the frequency of the vortex oscillation can be obtained from the linearized equation. Figure 4 shows the frequency as a function of applied magnetic in-plane field. Hysteresis is shown for a steep pinning potential, but the frequency

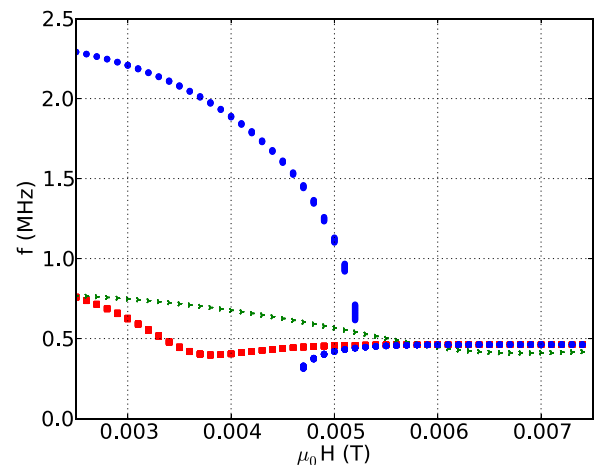


FIG. 4. Oscillation frequency as a function of applied magnetic in-plane field in the presence of one pinning center. The depinning is characterized by a minimum in frequency. For steep pinning potentials, hysteresis occurs. Pinning potential parameters: blue circles: $a = 2 \text{ eV}$ and $c = 7 \text{ nm}$, red squares: $a = 0.4 \text{ eV}$ and $c = 7 \text{ nm}$, and green triangles: $a = 2 \text{ eV}$ and $c = 17 \text{ nm}$.

increase is too high (2.3 GHz) compared with the experiments and former calculations.¹⁶ However, the shape of $f(H)$ is well reproduced in the measurement. An increase of about double the frequency (e.g., 790 MHz) is obtained by choosing the parameters of the pinning potential $a = 0.4$ eV and $c = 7$ nm. The hysteresis disappears in this case and the minimum frequency does not reach zero. The same is the case for increased c .

B. Micromagnetic simulations

In order to use a more realistic approach for comparison with the experiments, micromagnetic simulations were performed using the software package MuMax.¹⁷ A disk of 400 nm diameter is discretized using finite difference cells of $3.125 \times 3.125 \times 30$ nm³. Material parameters are $M_{\text{sat}} = 860$ kA/m, exchange stiffness $A = 1.3 \times 10^{-11}$ J/m², damping constant $\alpha = 0.02$ and no anisotropy. Following Ref. 2, we ascribed the distribution of pinning sites to the presence of material grains. Therefore, grains with average size of 10–30 nm (comparable to the disk thickness) were modeled using a Voronoi tessellation. We considered a reduced exchange coupling at the grain boundaries by reducing the exchange stiffness at the edges of the Voronoi regions by 20–40%. We excited small vortex core motions by applying perturbing in-plane spin-polarized electrical currents to the magnetic system, modeled following the Zhang-Li description.¹⁸ The amplitude of the current density was 5×10^9 A/m², large enough to cause vortex core displacements, but too small to cause depinning. After 40 periods of the excitation, the vortex core dynamics was considered to be in regime and the amplitude of the resulting oscillatory core displacements is recorded. When the excitation frequency corresponds to the resonance frequency, induced core displacements are much larger than off-resonance. For a grain size of 20 nm and an exchange reduction of 25% we obtain a frequency in the range of 700–1100 MHz when the vortex is pinned while it is decreased to 100–200 MHz when the vortex is depinned by field, which corresponds well to what is observed experimentally. The fact that the grain size is about the double of the distance between the pinning centers (frequency maxima) indicates that the vortex is pinned not only by pinning centers along a straight path from the disk center but also by all pinning centers (grain boundaries) that are next to this line (at a distance of half the grain size).

IV. CONCLUSION

We studied thermally excited vortex oscillations in Co-Fe-B MTJs affected by pinning centers experimentally, by analytic and micromagnetic modeling. We observed experimentally that at certain field values, steep frequency minima occur, which can be ascribed to flat regions in the energy landscape due to the applied field, which depins the vortex. This depinning can be hysteretic or non-hysteretic depending on how strongly the vortex is pinned (steepness of the pinning potential). In comparison with the experiments, the pinning potentials were estimated to be between -0.2 eV and -0.4 eV, and no hysteresis is observed. The average distances between the pinning centers were obtained to be 13 nm ($d = 460$ nm), 11 nm ($d = 590$ nm), and 7 nm ($d = 780$ nm). In the micromagnetic simulations, a different approach was used, taking into account the pinning centers as grain boundaries (20 nm grains) with reduced exchange interaction (25%), which leads to frequencies that are about double of the unpinned vortex oscillation frequency. The comparison indicates that the Thiele model can be applied; this means that the vortex in the presence of pinning centers remains sufficiently rigid.

ACKNOWLEDGMENTS

The research was funded by MIUR-PRIN 2010-11 Project No. 2010ECA8P3 DyNanoMag and EMRP JRP EXL04 (SpinCal). The EMRP is jointly funded by the EMRP participating countries within EURAMET and the European Union.

- ¹H. Min *et al.*, *Phys. Rev. Lett.* **104**, 217201 (2010).
- ²J. Leliaert *et al.*, *J. Appl. Phys.* **115**, 17D102 (2014).
- ³S. Parkin *et al.*, *Science* **320**, 190 (2008).
- ⁴A. Thiele, *Phys. Rev. Lett.* **30**, 230 (1973).
- ⁵M. Bryan *et al.*, *J. Phys. Condens. Mater.* **24**, 024205 (2012).
- ⁶J. Leliaert *et al.*, *Phys. Rev. B* **89**, 064419 (2014).
- ⁷R. Compton and P. Crowell, *Phys. Rev. Lett.* **97**, 137202 (2006).
- ⁸R. Compton *et al.*, *Phys. Rev. B* **81**, 144412 (2010).
- ⁹H. Min *et al.*, *Phys. Rev. B* **83**, 064411 (2011).
- ¹⁰A. Dussaux *et al.*, *Nat. Commun.* **1**, 1 (2010).
- ¹¹J. Schmalhorst *et al.*, *J. Appl. Phys.* **91**, 7478 (2002).
- ¹²K. Guslienko *et al.*, *J. Appl. Phys.* **91**, 8037 (2002).
- ¹³A. Khvalkovsky *et al.*, *Phys. Rev. B* **80**, 140401(R) (2009).
- ¹⁴T. Chen *et al.*, *Phys. Rev. Lett.* **109**, 097202 (2012).
- ¹⁵J. Burgess *et al.*, *Science* **339**, 1051 (2013).
- ¹⁶C. Zaspel, *Phys. Rev. B* **87**, 134425 (2013).
- ¹⁷A. Vansteenkiste *et al.*, *AIP Adv.* **4**, 107133 (2014).
- ¹⁸S. Zhang and Z. Li, *Phys. Rev. Lett.* **93**, 127204 (2004).